

Irena GUCWA, Tadeusz WIESER

The limburgites of the Polish Carpathians

The geochemical and petrographical correlation of mafic and ultramafic vulcanites and subvulcanites forming emplacements in Lower Cretaceous sediments of external and internal Carpathians was performed. Old and present analytical data yield further evidences implying consanguinity of Tatra limburgites with rocks of Silesian-Moravian teschenite formation. They represent products of initial volcanism connected with Neocimmerian tectonic phase. The limburgites seem to be probably first in succession, bounded to initial stages of rifting in continental crust of reduced thickness.

INTRODUCTION

Lately discovered occurrences of limburgites and augitites in association of other teschenite formation rocks in Bacharowice (S.W. Alexandrowicz et al., 1978), in borehole Sucha IG 1 (J. Strzępka et al., 1978) as well as of limburgite porphyries in Pastwiska, near Cieszyn (A. Mahmood, 1973) support the thesis of J. Morożewicz (1912) and S. Kreutz (1913) inferring the consanguinity of Silesian-Moravian picrites and teschenites (*sensu lato*) with contemporaneous Tatra limburgites.

Their petrogenetical definition has fundamental significance for evaluation and elucidation of the character and influence of Neocimmerian tectonic movements on the development of external Flysch Carpathians tectogene and deformations within the limits of Pieniny Klippen Belt and of Internal Carpathians (High and Low Tatra, High Fatra, Gerečse Mountains).

Exceptional position in these considerations occupy homogeneous and best, from the geological aspect, recognized Western Tatra limburgites.

Well known from his observation keenness Austrian geologist V. Uhlig, to whom we are indebted for discovery of multiple Carpathian vulcanites is as well the author (1897) of the first description of Western Tatra limburgites. His stable coworker, a petrographer C. John (*l. c.*) defined these rocks as diabases or diabase porphyrites. This diagnosis was verified by S. Kreutz (1913) who identified these vulcanites as limburgites. S. Kreutz's investigations conducted not only to the precise determina-

tion of mineralogical and chemical constitution but also revealed new occurrences, established synchronism and variability of structural-textural development, explained geological conditions of occurrence among other essential data. Specially important and noteworthy is the statement postulating a.o. the presence of tuffs (the term hyaloclastite was not yet introduced in the literature) and volcanic eruptions of supposedly submarine character.

F. Rabowski (1930) confirmed S. Kreutz's opinion of stable stratigraphic position of limburgites, and enlarged their spread. Besides, he accurately estimated the age as Lower Cretaceous basing on the presence of underlying *Calpionella* limestones. Further argumentation for mentioned conclusions was provided by Slovakian geologists and petrographers especially by V. Zorkovsky (1949), who, a.o. revealed the fact of occurrence of the crinoidal limestones in limburgite tuffites.

The problem of stratigraphic position of Tatra limburgites furthermore persisted as subject of interest, judging from later studies, conducted among Polish investigators particularly by Z. Kotański and A. Radwański (1959) and afterwards by J. Lefeld (1968). Formerly mentioned authors disclose the phenomena of rope-lava and crinoidal sediment mingling and after *Calpionella* and brachiopod (*Pygope diphya*) evidences improve age estimation to Lower Tithonian. Furthermore, they take also into consideration the symptoms of augmented in those times Neocimmerian tectonic activity synchronous with limburgite volcanism. Following other investigators in these movements they find the reason of cordillera uplifting, sea transgressions etc.

J. Lefeld (1968) modifies the age estimation of *Calpionella* limestones underlying limburgites accepting it as corresponding to latest Tithonian or Berriasian. But still remains as inadequately precised time of origin of *Globigerina* marls and younger cherts, overlying limburgites, what the establishment of upper age limit renders impossible. However, this writer suggests another solution in which the eruptions should took place in Berriasian or somewhat later.

Lately, Slovakian scientists, particularly D. Hovorka (1976), alone and in cooperation with J. Spišiak (D. Hovorka, J. Spišiak, 1981) reconsidered the problem of geological position of limburgites and magnified the knowledge of Tatra limburgite chemistry by many new determinations of macro- and microelements. After mentioned authors' opinion limburgites represent products of volcanic activity of the ocean island-type, characterized by the preponderance of hyaloclastites over lava flows. The basement complex presented there a crust of transitional type and intensive assimilation processes modified indistinctly alkaline and under-saturated volcanics character. They also propose another more suitable name for Tatra limburgites in the form of A. Streckeisen's (1978) term – hyalobasanite. However, according to J. Nicholls et al. (1982) for the use of basanite term indispensable is rather high content of normative nepheline, surpassing 5 per cent, not own to the Tatra limburgites.

Another known area of limburgite occurrences is contained within the extent of petrographic, Silesian-Moravian, teschenite formation. The presence of limburgites in this association already was announced by O. Pacak (1926) and later by K. Smulikowski (1929), when he emphasizes (p. 31) the similarity of a melanocratic rock of lamprophyre-type from Marklowice with some limburgites. Likewise, noteworthy is the occurrence near Teschen (Pastwiska) reported by A. Mahmood (1973) as a sill of limburgite porphyry, exhibiting transitional structural features to monchikite-like lamprophyre.

To the structurally proper limburgite, strictly augitite (when taking into account the preponderance of clinopyroxenes), should be included a mandelstone and

associated hyaloclastites, found in a block of many metres in diameter. It is contained (see S.W. Alexandrowicz et al., 1978) in Upper Miocene (Lower Badenian) molasse in Bacharowice (12 km NE of Wadowice).

Petrographically much resembling those from Bacharowice are some up to twenty cm. large rounded, redeposited fragments of also amygdaloidal varieties, found in borehole Sucha IG 1 (J. Strzépka et al., 1978). The age of confining sediments is Lower Miocene, older than Carpathian-Ottngian.

LIMBURGITE OF OSOBITA MASSIF

Detailed S. Kreutz's description (1913) yields numerous instances of solid limburgite and of limburgite tuff (now classified as hyaloclastite), which should be in whole measure acknowledged as representative and as such utilized in correlation as exemplary. This is well expressed in petrographic and geochemical studies of D. Hovorka and J. Spišiak (1981) embracing six complete chemical analyses as well as in now presented two analyses of amygdaloidal limburgites from Bobrowiecka Pass (sample no. 1) and Osobita massif (sample no. 2).

Amygdaloidal limburgites of Osobita display oligophyric structure of seriate type, where the phenocryst fraction constitutes clinopyroxene, while microphenocryst one – clinopyroxene and olivine pseudomorphs. Microlites are represented by clinopyroxene, titanomagnetite and apatite. Clinopyroxenes exhibit, an euhedral habit which in microlite generation more frequently corresponds to subhedral one. Among observed simple forms the most common are: $\{110\}$, $\{100\}$, $\{010\}$ and $\{\bar{1}11\}$. Zoning and hour-glass structure showing joined $\{\bar{1}11\}$ growth sectors are well accentuated. Simple twins after $\{100\}$ planes are quite common. The optical properties indicate varying titanium content in a ferroaugite-type clinopyroxene. The content of this element increases systematically, especially in $\{100\}$ growth sectors, judging from rising values of $2V_v$, from 54° to 59° with distinct dispersion $r > v$, of extinction angles γ/c from 41° to 54° and of increasing rose-violet absorption. The refractive indices for $\{\bar{1}11\}$ growth sector amount: $n_v = 1.736$, $n_b = 1.718$, $n_a = 1.712$ and indicate together with $2V_v$ titaniferous ferroaugite composition (Fig. 1).

Olivines, strictly their calcite pseudomorphs with subordinate chlorophite admixture, are observed only as microphenocrysts, reaching up to 0.5 mm in diameter. Their contours are subhedral, through the appearance of more or less marked, simple forms, as: $\{010\}$, $\{011\}$, $\{110\}$, $\{101\}$ and $\{021\}$.

No plagioclase microlites were discerned. Numerous isometric grains of titanomagnetite are anhedral and relatively small and variable in size. Infrequent apatite has a shape of small needles. Among secondary minerals predominates calcite, forming veinlets, infilling vesicles and replacing olivine grains. The vesicles are sometimes filled by septechlorites and albites (usually taken as zeolites – Table 1, Fig. 15); the mineral succession is as follows: septechlorite \rightarrow albite \rightarrow calcite. The content of amygdales in rock varies between some to 50 vol. per cents, and their diameter – from 0.6 up to 3 mm.

Another specimen (no. 1) of amygdaloidal limburgite from Bobrowiecka Pass differs against former variety by larger size of olivine pseudomorphs, higher frequency of clinopyroxene grains forming glomerophyric segregations, higher content of apatite, and more often demonstrated infilling of vesicles by septechlorite and albite (Table 1, Fig. 14).

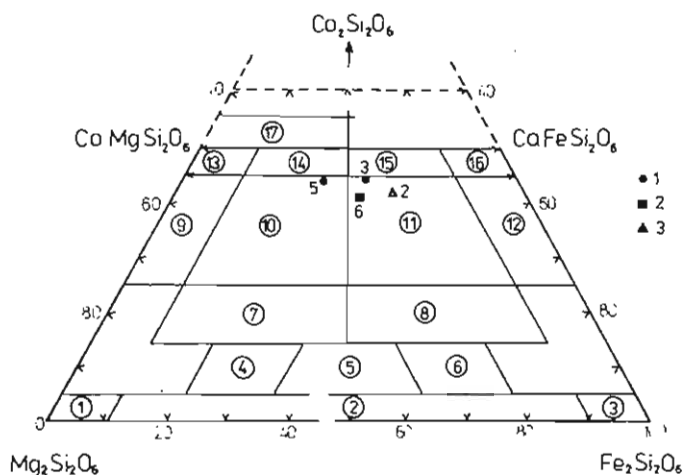


Fig. 1. Slightly modified A. Poldervaart's and H. Hesse's (1951) classification diagram of clinopyroxenes showing chemistry of examined and compared limburgite augites after optic axial angles and refractive indices data

Diagram klasyfikacyjny klinopiroksenów, nieco zmodyfikowany przez A. Poldervaarta i H. Hessa (1951), przedstawiający chemizm badanych i użytych do porównań aigitów z limburgitów, na podstawie kątów osi optycznych i współczynników załamania światła

1 – samples nos 3 and 5 from Bacharowice (see Table 1); 2 – sample no. 6 analyzed by S. Kreutz (1913) – see Table 2; 3 – sample no. 2 from Osobita (see Table 1); numbers in circles a.o. denote: 10 – proper augite, 11 – ferroaugite
1 – próbki nr 3 i 5 z Bacharowice (patrz tab. 1); 2 – próbka nr 6 analizowana przez S. Kreutza (1913) – patrz tab. 2; 3 – próbka nr 2 z Osobitej (patrz tab. 1); numery w kółkach m. in. oznaczają: 10 – aigit właściwy, 11 – ferroaigit

LIMBURGITE-LIKE ROCKS OF BACHAROWICE AND SUCHA

Primarily recognized as a dike (S.W. Alexandrowicz, W. Heflik, 1974) in reality over two metres large block (S. W. Alexandrowicz, et al., 1978) is polygenetic, that is composed of a number of smaller blocks and pebbles. The largest one is formed by a mandelstone, containing inside a smaller fragment of hyaloclastite. The mandelstone (sample no. 5) has been undergone to multiple alterations including: nontronitization, saponitization, calcitization, a.o. under the influence of post-magmatic hydrothermal solutions and hot sea water. The montmorillonitization could take place mainly in connection with the meteoric water circulation, before and after deposition (actual weathering) amidst Miocene molasse sediments. In the least transformed parts of mandelstone the reconstruction of primary mineral constitution is still feasible.

The common essential component, augite in peripheral parts of grains provides the optical properties corresponding to titaniferous ferroaugite, basing on the following variability of optical data: $2V_{\gamma} = 48^{\circ} - 48.5^{\circ}$ (in $\{100\}$ growth sector) and $53^{\circ} - 57^{\circ}$ (in $\{\bar{1}11\}$ growth sector), while γ/c equals 53° and $43.5^{\circ} - 48^{\circ}$, respectively. The refractive indices measured for internal parts of $\{100\}$ sectors amounted as follows: $n_{\gamma} = 1.720 \pm 0.001$, $n_{\delta} = 1.700 \pm 0.002$, and $n_{\alpha} = 1.695 \pm 0.001$; whereas optic

axes angles, $2V_\gamma$, reached up to 53° (Fig. 1). The clinopyroxene grain may commonly be overgrown by a barkevikite with features much approximating the lamprobolite own, as: $\gamma/c = 14^\circ$, $2V_\alpha = 67^\circ$, strong pleochroism, showing for γ – dark red-brown, β – dark brown with red hue, α – yellowish colours. It is quantitatively subordinate in relation to clinopyroxene (15 and nearly 50 per cents, resp.). The serpentine-saponite pseudomorphs (\pm calcite) after olivine, titanomagnetite (nearly 10 per cent) in skeletal crystals, variously albitized plagioclase (formerly labradorite with An_{51-52}), in aggregates resembling variolitic ones, needle-like apatite and pyrite supplement the list of primary mineral constituents. The glass is replaced here by analcite, rarer natrolite, as well as by chlorite and nontronite. In vesicles, attaining the diameter of up to 2.25 mm and constituting up to a little over 15 per cent by volume, occur the following paragenetic assemblages of secondary minerals (inwards): nontronite-quartz-nontronite-analcite-nontronite-saponite, or nontronite-analcite-calcite-ankerite-nontronite-saponite, or ankerite-saponite, or ankerite-nontronite-calcite, or nontronite-calcite. The calcite and ankerite were additionally noted as infillings of rare and thin veinlets.

The quantitative proportions of minerals and structural-textural features induce to the acceptance of the term – melabasalt or picrite basalt. The last name is here used only in *sensu lato* meaning that is with preponderant augite, since some authors give equality signs for picrite basalts and olivine-rich oceanites. In relation to limburgites and augitites they deviate a little owing to glass scarcity and plagioclase presence.

For described rocks the origin as product of submarine eruption is assumed. This is argued not only through the existence of specific amygdales and kind of secondary minerals in solid lava but also the co-occurrence (in this same block) with hyaloclastes (Table II, Fig. 17; Table III, Figs. 18–19). The last mentioned variety is composed of glass shards sometimes in 80 and more per cents altered in chlorite (chloropheite), either in association with smectite (nontronite-saponite and montmorillonite) or not, but always with calcite admixture. The calcium carbonate appears also in authigenic, rhombohedral calcite crystals of up to 0.1 mm in diameter, two times smaller than palagonitized and further altered, as above, glass shards. Accordingly with increasing marly matrix content poikiloclastic (or Fontainebleau-type) texture may develop.

Independently found another, but much smaller block (30 × 40 cm in diameter, sample no. 3) is composed of a rock showing mineral and structural-textural features close to those characterizing biotite monchiquite and limburgite. Supposedly derived from interior of a lava flow or from a sill it abounds in clinopyroxene (up to 49 per cent) in form of large megacrysts (up to 4.5 mm in diameter), poikilitically intergrown by glass, and microlites as well. The optical properties of clinopyroxene phenocrysts can change due to zoning and hour-glass structure as follows: $2V_\gamma = 57^\circ$ and $\gamma/c = 48.5^\circ$ for $\{111\}$ growth sector, or $2V_\gamma = 55^\circ$ and $\gamma/c = 56^\circ$ for $\{100\}$ growth sector, in mean values. The mean refractive indices equalled: $n_\gamma = 1.730$, $n_\beta = 1.710$, $n_\alpha = 1.705$. In microlites: $2V_\gamma = 55^\circ$ and $\gamma/c = 48.5-51^\circ$. The place of barkevikite in this rock occupies biotite, constituting 5 per cent of rock by volume. The optic data, like $2V = 0^\circ$ and $n_\gamma = n_\beta = 1.624$ indicate low iron content (phlogopite chemistry). The pseudomorphs after olivine (up to 10 vol. per cent), titanomagnetite, pyrite, apatite and sporadic zircon were also noted. From secondary minerals mention worthy is the occurrence of chlorite-saponite association filling rare and small vesicles (up to 0.8 mm across) and of natrolite with rare chlorite as glass replacement products.

In borehole Sucha IG 1, at 2818.35 m depth were also found amygdaloidal

Table 1

Chemical composition of limburgite and limburgite-like rocks in weight per cents

Component	1	2	3	4	5
SiO ₂	35.73	33.64	39.66	38.82	36.95
TiO ₂	3.42	4.42	3.76	4.59	3.27
Al ₂ O ₃	11.58	11.79	11.02	13.05	13.79
Fe ₂ O ₃	11.00	9.99	4.28	10.76	8.81
FeO	5.96	6.16	7.11	14.92	11.23
MnO	0.18	0.20	0.06	0.03	0.09
MgO	3.59	4.10	11.79	6.29	4.63
CaO	15.49	16.56	12.83	3.52	9.64
Na ₂ O	1.99	0.65	0.33	0.68	0.48
K ₂ O	1.23	1.47	3.00	0.96	0.84
P ₂ O ₅	0.07	0.06	0.35	0.06	0.69
CO ₂	5.33	5.92	—	—	2.20
S	0.07	0.06	—	—	—
H ₂ O ⁺	2.33	2.75	2.61	2.91	1.67
H ₂ O ⁻	1.61	1.69	3.02	1.79	4.50
Total	99.58	99.46	99.82	99.38	98.79

1, 2 — limburgites, Osobita, West High Tatra; 3, 5 — limburgite-like rocks of Bacharowice; 4 — limburgite-like rock from Sucha IG 1 borehole (depth: 2818.35 m). Analyst: I. Gucwa

limburgites or their augite-rich varieties — augites, embedded in Miocene molasse deposits. Roundstones up to 8 cm large show many similarities in petrographic and chemical constitution, if confronted with those just recorded for Bacharowice blocks.

CHEMICAL CHARACTERISTIC OF DESCRIBED ROCKS

The chemical investigations executed on presented limburgite-type rocks consisted of the definition of bulk chemical composition of rocks and of determination of selected trace elements. From the last mentioned, special emphasis was directed on the determination of such microelements as V, Cr, Ni, Co, Cu, Mn, known from their abundance in mafic minerals in early stages of differentiation of basaltoid magmas (A. Polański, K. Smulikowski, 1969). Furthermore, these metals, especially Cr, Ni, and Ti characterizes distinct content decrease with SiO₂ increase. They are utilized as indicative in magmatic differentiation sequences from ultramafic to salic rocks.

For chemical characteristic the results of bulk chemical analyses of two Osobita limburgites, two limburgite-like rocks from Bacharowice and one from Sucha IG 1 borehole were used. The results of macroelement determinations with localization of samples are listed in Table 1. The results of selected published chemical analyses of Silesian „teschenite formation” rocks (K. Smulikowski, 1929; A. Mahmood, 1973) and Osobita limburgite (S. Kreutz, 1913), are independently tabulated

Table 2

Chemical composition of similar rocks used for comparison in weight per cents

Component	6	7	8	9	10	11	12	13
SiO ₂	41.43	50.41	49.00	47.20	43.40	39.73	39.38	38.90
TiO ₂	2.73	0.55	2.28	2.22	1.03	2.15	1.73	1.50
Al ₂ O ₃	11.73	22.60	14.67	18.92	9.77	12.46	7.64	12.48
Fe ₂ O ₃	11.38	1.20	1.97	3.83	4.49	3.73	4.97	6.30
FeO	5.86	2.74	7.14	5.60	5.30	7.19	7.23	4.16
MnO	0.43	0.11	0.14	0.16	0.05	0.18	0.17	0.05
MgO	7.43	0.55	6.69	3.05	11.45	8.26	22.05	12.55
CaO	11.43	6.48	9.43	7.86	14.15	14.72	8.62	15.00
Na ₂ O	3.29	4.23	3.56	4.45	0.60	2.39	0.43	1.76
K ₂ O	0.48	5.75	1.88	2.80	0.93	1.83	1.12	0.66
P ₂ O ₅	0.39	0.16	0.39	0.69	0.46	1.00	0.44	1.00
CO ₂	0.55	—	0.49	—	0.60	3.00	—	1.25
S	—	tr.	0.12	0.05	—	0.19	0.07	—
H ₂ O ⁺	2.52	4.90	2.31	3.06	7.23	3.28	4.93	4.46
H ₂ O ⁻	0.28	0.26	0.32	0.34	—	0.29	0.95	—
Total	99.93	99.94	100.39	100.23	99.46	100.40	99.73	100.07

6 – limburgite, Sucha Valley, West High Tatra (S. Kreutz, 1913); 7 – nepheline syenite, Puńców near Teschen (K. Smulikowski, 1929); 8 – diabase-dolerite, Boguszowice near Teschen (K. Smulikowski, 1929); 9 – essexitic teschenite, Dzięgielów near Teschen (K. Smulikowski, 1929); 10 – limburgite porphyrite, Pastwiska near Teschen (A. Mahmood, 1973); 11 – melanocratic monchiquite, Grodziec near Teschen (K. Smulikowski, 1929); 12 – picrite, Moravia, (Starič *vide* K. Smulikowski, 1929); 13 – limburgite porphyrite, Pastwiska near Teschen (A. Mahmood, 1973)

(Table 2). The analyses are ordered according to the decreasing SiO₂ content in similar rocks. Introduced numeration of samples was also applied in the graphic representations.

The bulk chemical analyses of chief constituents were performed as other wet classical analyses.

The results of chemical analyses have been undergone to various well known calculation techniques. From these some are specially convenient to interpretation of the obtained results. They include even, until now useful P. Niggli's (1936) numbers and CIPW (Fig. 2) norms – normative mineral contents, well suitable for characterization of magmas and for further calculations.

A common feature for investigated rocks is their basic character, emphasized by undersaturation in silica (Niggli's group IV), expressed by parameter $q = -12$ to -50 .

The differentiation trends in rocks under examination are well illustrated by the proportions and compositions of normative minerals plotted on diagram (Fig. 2). It allows to discern, in dependence of silica saturation grade and share of mafic constituents – three groups of rocks, namely:

1. Most undersaturated, alkaline varieties characterized by the presence of normative nepheline (1–5 per cent), are represented by limburgite-like rock of Bacharowice (3), diabase of Boguszowice (8) and S. Kreutz's (1913) limburgite of Osobita (6).

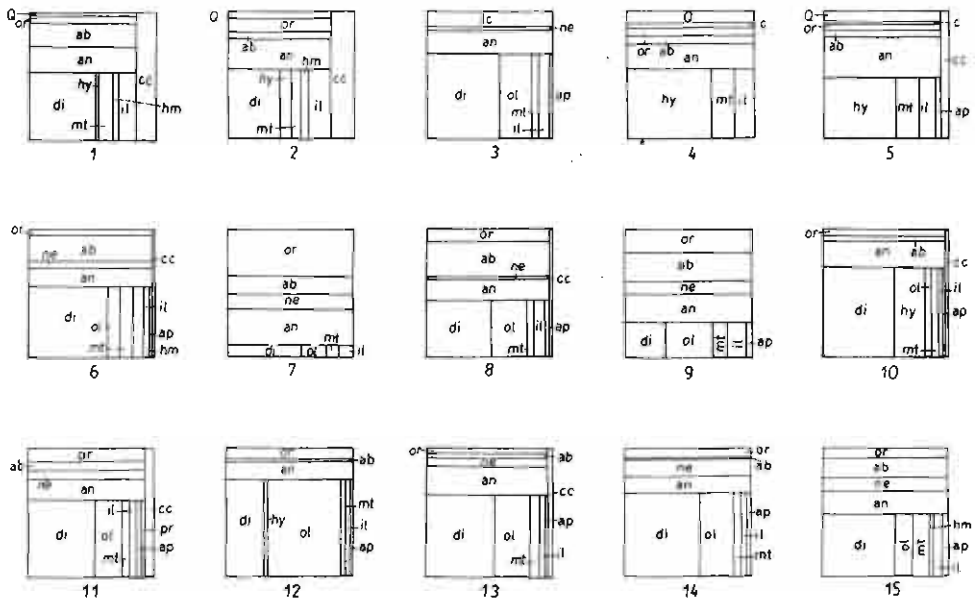


Fig. 2. Diagrams illustrating normative mineral compositions (after CIPW method of calculations) and quantitative proportions in examined limburgites and comparable related rocks

Diagramy ilustrujące normatywny skład mineralny (według metody CIPW) i ilościowe proporcje w analizowanych limburgitach i porównywalnych, pokrewnych skalach

1 - 13 - limburgites and selected rocks of teschenite formation of Silesia and Moravia, numbered as in Tables 1 and 2; 14 - average limburgite after R.A. Daly (1933); 15 - average augitite after R.A. Daly (*l.c.*)

1 - 13 - limburgity i wybrane skały formacji cieszyniowej Śląska i Moraw, numeracja jak na tab. 1 i 2; 14 - średnia dla limburgitów według R.A. Daly'ego (1933); 15 - średnia dla augitytu według R.A. Daly'ego (*l.c.*)

2. Varieties with lacking nepheline and containing beside olivine, rather large quantities of normative hypersthene but without appearance of normative quartz. They include some rocks of Silesian-Moravian teschenite formation, like picrite (12), limburgite-like rock from Pastwiska (10).

3. The last group of rocks embraces Osobita limburgites (1,2), limburgite-like rocks of Bacharowice (5), and Sucha (4) which together with normative hypersthene prove to contain some mol. per cents of normative quartz. This is interpreted as the result of secondary transformations of rocks.

T. Barth's (1948) method of calculations is helpful in the establishment of element balance, especially in the interpretation of secondary alteration processes in examined rock. Basing on this calculations whose results are comprised in Table 3, special triangular diagram for major cations (Fig. 3a, b, c), were constructed.

On the diagram Na - K - Ca (Fig. 3a) noteworthy is the stable and rather high content of potassium in limburgites and limburgite-like rock of Sucha if confronted with a little lower values for rocks of teschenite formation. The differences among limburgites and compared rocks are due to the changes of relation Ca:Na, connected with secondary metasomatic processes (e.g., calcitization).

The diagram Fe - Ca - Mg (Fig. 3b) allows to disclose a distinct partition into Mg - Ca - Fe varieties comprising limburgite-like rock of Bacharowice (3), diabase

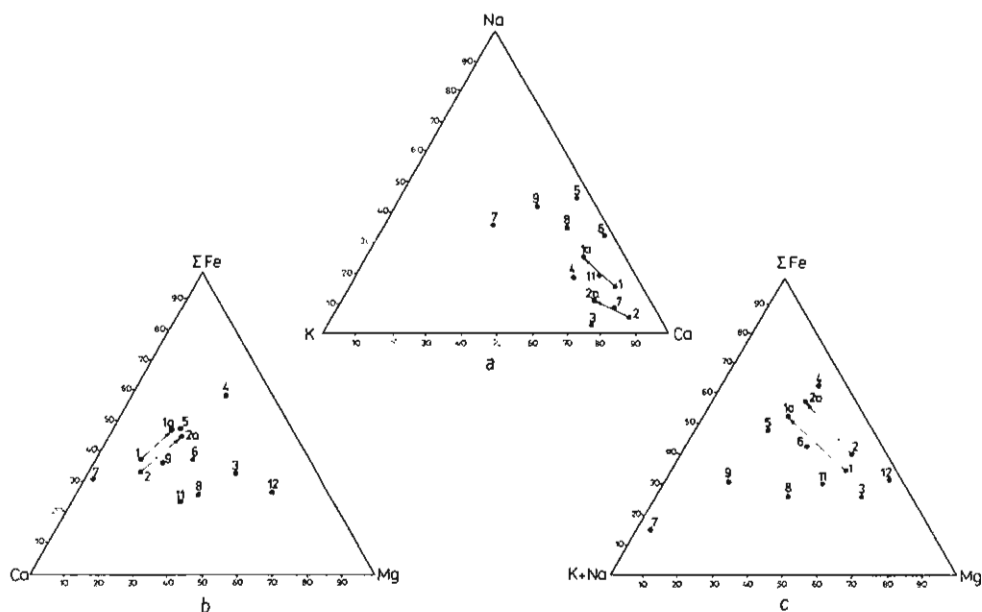


Fig. 3. Triangular projections of major (petrogenic) element relations as Na - K - Ca (a), Fe (total) - Ca - Mg (b) and Fe (total) - K + Na - Mg (c)

Trójkątne diagramy głównych (petrogenetycznych) pierwiastków dla stosunków Na - K - Ca (a), Fe (całkowite) - Ca - Mg (b) i Fe (całkowite) - K + Na - Mg (c)

Numbers repeat the numeration of samples given in Table 1 and 2, and in Fig. 2; numbers 1a and 2a correspond to 1 and 2 respectively, after subtraction of Ca contained in carbonates

Numery próbek jak w tab. 1 i 2 i na fig. 2; numery 1a i 2a odpowiadają numerom 1 i 2, po odjęciu Ca związanego w węglanach

of Boguszowice and Moravian picrite, Ca - Fe - Mg varieties of Osobita limburgites (1,2), and Fe - Mg - Ca ones including limburgite-like rocks of Sucha (4) and Bacharowice (5). To the projection points of lately mentioned rocks may be brought closer the points (1a,2a) plotted after subtraction of CaCO_3 from analyses of Osobita limburgites (1,2), implying the consanguinity of these rocks (compare also Fig. 2).

The diagram Fe - Na + K - Mg (Fig. 3c) visualizes the stable quantity of magnesium in Osobita limburgites, and simultaneously variable relation of alkalis to iron. After elimination of calcium carbonate from the composition of Osobita limburgite (projection points 1a, 2a) also in this case the relationship of Osobita, Bacharowice, and Sucha limburgites and limburgite-like rocks becomes quite evident.

On the all three diagrams differentiation orders for Osobita limburgites and related limburgite-like rocks might be established, as well as chaotic dispersion of teschenite formation rocks plottings.

Similar remarks appear after comparison of projection point positions on diagram constructed after H. Kuno et al. (1957), basing on the distribution of chief rock components according to crystallization quotient, $\text{CQ} = \frac{100 \text{ MgO}}{\text{MgO} + \text{FeO} + \text{Fe}_2\text{O}_3 + \text{Na}_2\text{O} + \text{K}_2\text{O}}$ (Fig. 4).

Equally limburgite-like rocks from Bacharowice (5) and Sucha (4), as well as Osobita limburgite (1,2), distinguishes low crystallization quotient. Instead, the

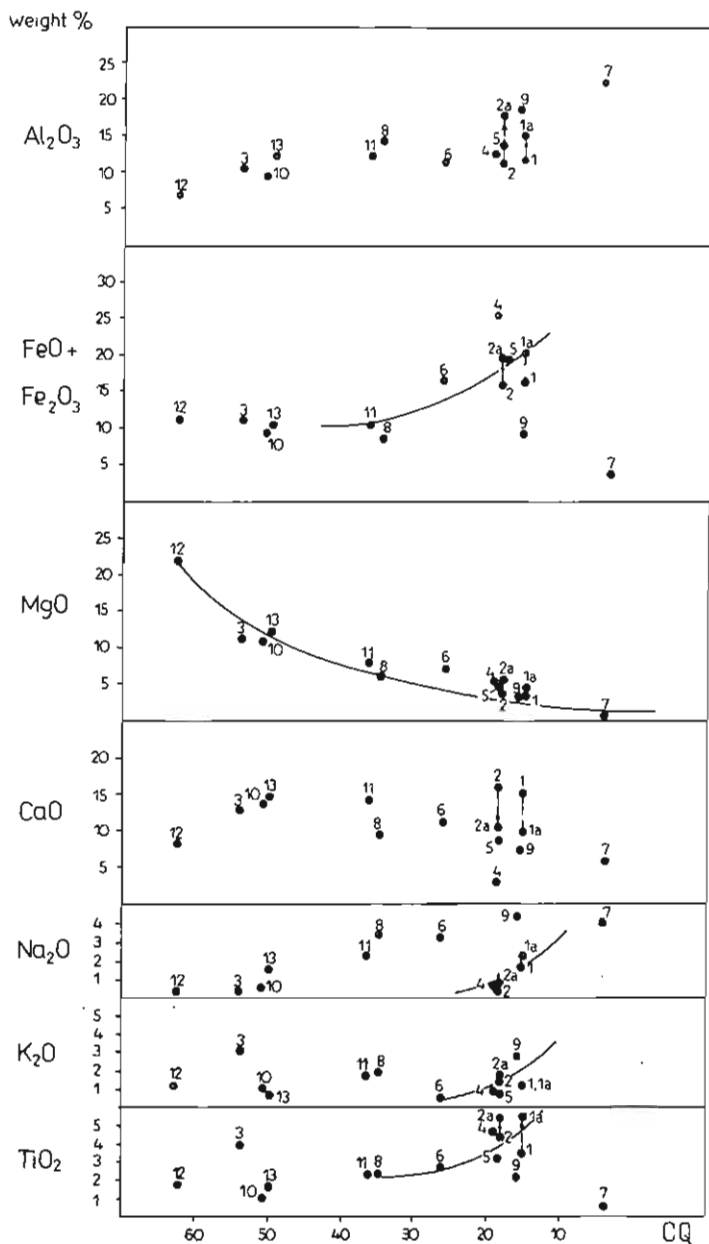


Fig. 4. The contents of main oxide components of rock (in weight per cents) versus crystallization quotient (CQ) = $100 \text{ MgO}/\text{MgO} + \text{FeO} + \text{Fe}_2\text{O}_3 + \text{Na}_2\text{O} + \text{K}_2\text{O}$

Zawartości głównych składników tlenkowych skal (w procentach wagowych) w stosunku do wskaźnika krystalizacji (IK) = $100 \text{ MgO}/\text{MgO} + \text{FeO} + \text{Fe}_2\text{O}_3 + \text{Na}_2\text{O} + \text{K}_2\text{O}$

Explanations as given in Fig. 3

Objaśnienia jak na fig. 3

CQ of teschenite formation representatives incline toward higher values. Extremal position on diagram occupies an ultramafic Moravian picrite (12) and a most salic, nepheline syenite (7). In the plotting area of limburgite and limburgite-like

Table 3

The Barth's parameters of examined rocks
O(OH) = 160

Sample no.	K	Na	Ca	Mg	Fe ²⁺	Fe ³⁺	Mn	Al	Ti	Si	P	C	S	O	(OH) 16.0
1	1.5	3.7	16.0	5.1	4.8	8.0	0.1	13.2	2.5	36.7	0.1	7.0	0.1	145.7	14.3
2	1.9	1.2	17.5	6.0	5.1	7.4	0.2	13.7	3.3	33.2	—	8.0	0.1	142.8	17.2
3	3.9	0.6	13.9	17.8	6.0	3.3	0.1	13.2	2.9	40.2	0.3	—	—	143.4	16.6
4	1.2	1.3	4.3	9.6	12.8	8.3	—	15.8	3.3	39.8	0.1	—	—	141.3	18.7
5	1.1	9.7	10.8	7.2	9.8	6.9	0.1	16.9	2.6	38.5	0.6	3.1	—	149.2	10.8
6	0.6	6.3	12.0	10.9	4.8	8.4	0.4	13.6	2.0	40.7	0.3	0.7	—	144.1	15.9
7	6.6	7.4	6.3	0.7	2.1	0.8	0.1	24.1	0.4	45.6	0.1	—	—	132.0	28.0
8	2.2	6.4	9.5	9.3	5.6	1.4	0.1	16.2	1.5	45.8	0.3	0.6	0.2	145.9	14.1
9	3.3	8.1	7.9	4.2	4.4	2.7	0.1	20.9	1.6	44.2	0.5	—	0.1	141.5	18.5
11	2.2	4.4	15.0	11.7	5.7	2.7	0.1	14.0	1.5	37.8	0.8	3.9	0.3	139.8	20.2
12	1.3	0.8	8.4	29.8	9.5	5.5	0.1	8.2	1.2	35.7	0.3	—	0.1	132.0	28.0

For number of samples see Table 1 and 2

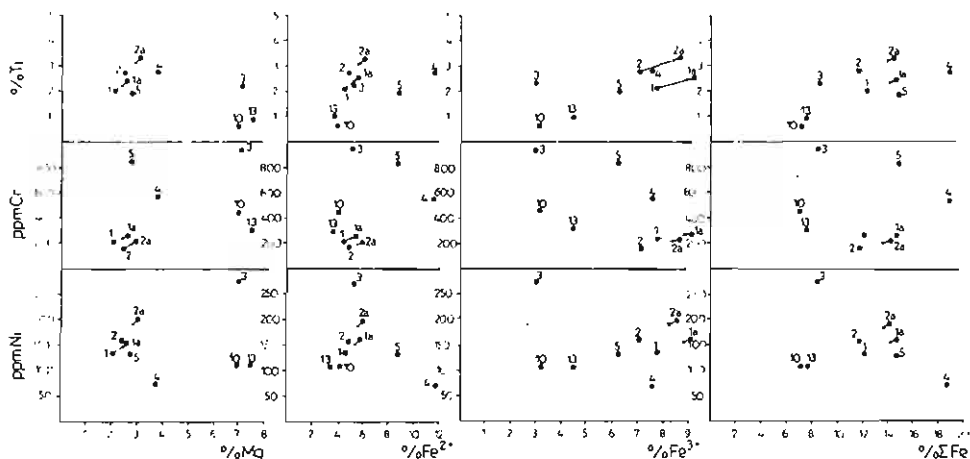


Fig. 5. The dependences between TiO_2 (in weight per cents), Cr and Ni (ppm) and mafic element (Mg, Fe^{2+} , Fe^{3+} , total Fe) contents

Zależności między TiO_2 (w procentach wagowych), Cr i Ni (g/t) a pierwiastkami maficznymi (Mg, Fe^{2+} , Fe^{3+} , Fe całkowite)

Explanations as given in Fig. 3

Objasnienia jak na fig. 3

rocks some trends consisting of an increase in TiO_2 , $\text{FeO} + \text{Fe}_2\text{O}_3$, Na_2O and K_2O contents with decrease of crystallization quotients are revealed. On the other hand, the decrease of MgO content with reduction of this quotient involves all the assemblage of projection points, including those of teschenite formation. This makes evident the course of differentiation processes from highly mafic varieties, represented by Moravian picrite to salic ones, as nepheline syenite.

The results of trace elements determinations in ppm are demonstrated in Table 4, together with analytical results for some selected main elements in weight per cents. Due to the restricted quantity of available analytical material in some cases statistical methods were replaced by graphic presentations. These embrace the dependences of microelement versus macroelement contents (Fig. 5), the relations between Cr, Ni, and Ti abundance and the values of Niggli's mg parameters (Fig. 6), and the interdependences between defined microelements (Fig. 7).

The considerations regarding the concentrations of microelements in analyzed rocks lead to the following generalizations:

Titanium – detected in amounts ranging from 0.61 up to 2.75 per cents, highest values attains in limburgite-like rocks of Sucha and Bacharowice and a little lower in Osobita limburgites. Exhibited (Fig. 6) relations between Ti and mg parameter induce distinct partition into two populations, depending from mg parameter: one – embracing points for Osobita (1,2), Bacharowice (3,5) and Sucha (4) rocks, second – points for Pastwiska limburgite-like rocks of teschenite formation (10,13), characterized by higher mg values.

This partition of titanium has its reason in greater affinity of titanium to iron, especially if trivalent (Fig. 5). This is evidenced by the enrichment of final basaltic magma differentiation products with both metals. Further positive correlations were disclosed also for other pairs of metals enriched in basic rocks, as: Ti–Cr; Ti–Ni and Ti–Mn. Most distinctly they are shown in limburgitic rocks from

Table 4

Selected macro- and microelements content in limburgite and limburgite-like rocks

Sample no.	Percentage					Content in ppm					
	Fe ²⁺	Fe ³⁺	Fe	Mg	Ti	Cr	Ni	Co	V	Mn	Cu
1	4.63	7.69	12.32	2.17	2.05	218	136	125	—	1811	435
1a	5.55	9.21	14.76	2.59	2.45	262	163	150	—	2173	522
2	4.79	6.99	11.78	2.47	2.65	184	161	14	—	1963	1445
2a	5.87	8.57	14.44	3.05	3.25	226	198	17	—	2414	1777
3	5.50	2.99	8.49	7.11	2.25	970	275	6	n.d.	631	672
4	11.60	7.53	19.13	3.79	2.75	560	72	8	n.d.	272	2740
5	8.73	6.16	14.89	2.79	1.95	818	136	8	n.d.	897	635
10	4.12	3.14	7.26	6.91	0.61	465	115	—	285	n.d.	45
13	3.23	4.41	7.64	7.57	0.90	320	110	—	520	n.d.	110

Numeration as in Table 1 and 2; 1a = 1 recalculated after subtraction of calcium carbonate; 2 = 2a as for 1a = 1

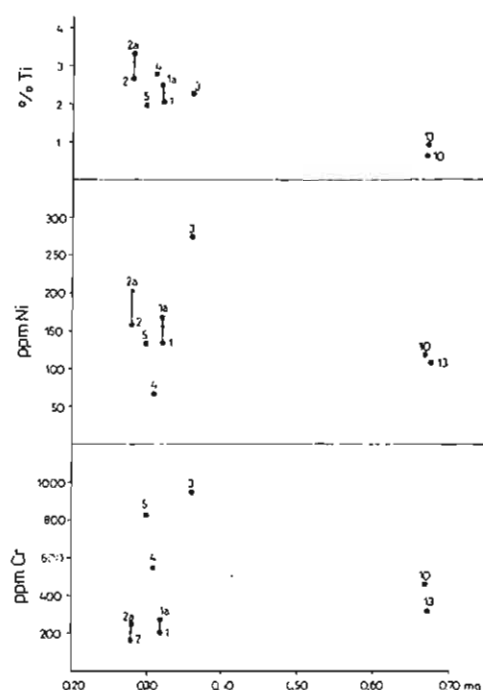


Fig. 6. The relations between Ti, Ni, Cr abundances and Niggli's mg parameter variations
Stosunki między nagromadzeniem Ti, Ni, Cr a zmiennością parametru mg Niggli'ego

Explanations as given in Fig. 3

Objaśnienia jak na fig. 3

Osobita, Bacharowice and Sucha. Less conspicuous relation could be observed in rocks from Pastwiska (Fig. 7).

Chromium — like titanium, is especially concentrated in samples from Bacharowice (3,5) and Sucha (4), where the Cr contents were noted reaching from 560 up to 970 ppm. Instead, in Osobita limburgite they never surpass 218 ppm, the quantity which can be augmented to 262 ppm when calcium carbonate is excluded and the rest is recalculated to 100 per cent. Substantial enrichment in chromium of limburgite-like rocks from Bacharowice and Sucha stays probably in connection with the enrichment in iron, especially divalent, showing with this metal and magnesium positive correlation (Fig. 5). This interdependence is well marked by the distribution of projection points in Fig. 6, demonstrating as in titanium case separate populations containing Osobita, Bacharowice and Sucha samples against Pastwiska samples. Other positive correlation examples comprise: Cr—Mn, Cr—Ti and Cr—Ni pairs (Fig. 7).

Nickel — as formerly cited titanium and chromium attains maximal concentrations in Bacharowice (3, 5) samples (275 and 136 ppm, respectively) and Osobita (1, 2) samples (136 and 161 ppm resp.). The lowest values were obtained for Pastwiska samples (115 and 110 ppm). In all rocks a distinct positive correlation for Fe^{2+} —Ni (Fig. 5), Ni—Cr and Ti—Cr pairs was stated (Fig. 7). The last mentioned dependences are well noticeable in Fig. 5, with projection points grouped in a single population.

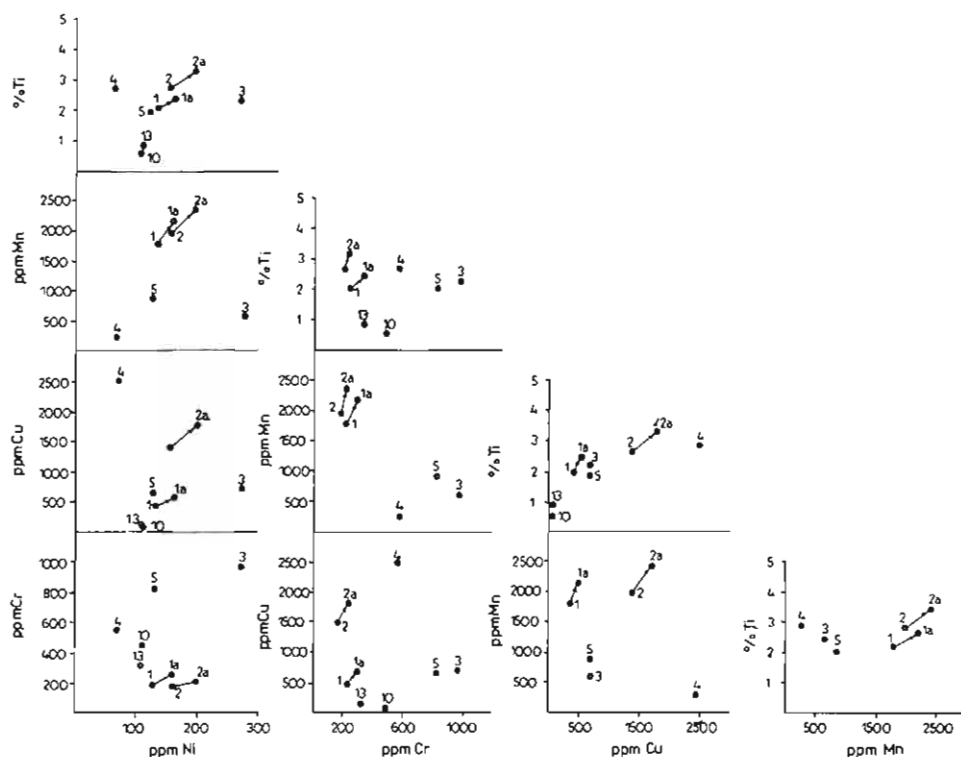


Fig. 7. The mutual relations between selected microelements as Cu, Cr, Ni and Ti, Mn
Wzajemne stosunki między wybranymi mikroelementami, jak Cu, Cr, Ni oraz Ti i Mn

Explanations as given in Fig. 3

Objaśnienia jak na fig. 3

C o b a l t — enriched only in one sample from Osobita. The remaining occur in amounts not exceeding 14 ppm.

V a n a d i u m — does not reveal any remarkable differences useful for comparisons.

M a n g a n e s e — largest concentrations of this metal were noted in Osobita limburgites (1811–1963 ppm). Positive correlations revealed in Cr–Mn and Ti–Mn pairs (Fig. 7) indicate the common provenance of elements.

To sum up considerable enrichment in titanium, chromium and nickel own for highly basic magmas should be emphasized. Similar high quantities of metals are reported from Slovakian limburgites (D. Hovorka, J. Spišiak, 1981). They oscillate in the same limits, as, e.g., in Osobita limburgites (TiO₂—3.63 per cent. Ni—163 ppm, Cr—179 ppm, Mn—1500 ppm).

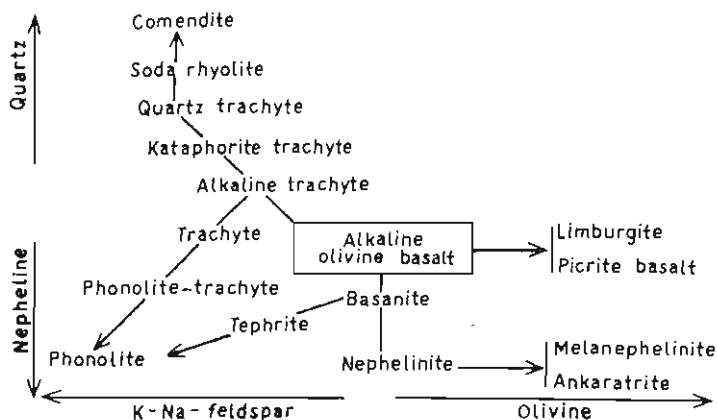


Fig. 8. Differentiation trends of Kenya alkaline volcanics, after E.P. Saggerson (1970)
Trendy dyferencycyjne w wulkanitach alkalicznych Kenii według E.P. Saggersona (1970)

COMPARISONS AND CONCLUSIONS

The term – limburgite was at first introduced in world literature by H. Rosenbusch in 1872 to define a highly glassy effusive rocks with olivine and augite phenocrysts. Its name was derived from a small town Limburg situated near volcanic massif of Kaiserstuhl, within the limits of Rhenish tectonic trough. There it occurs as small magmatic, volcanic and subvolcanic, bodies in an assemblage comprising also more or less alkaline rocks.

The limburgites, in the sense in which this name was used in popular handbook written by Williams, Turner and Gilbert, they represent ultramafic rocks which form lava flows, dykes, sills and domes. They are usually accompanied by alkaline rocks, particularly analcite basanites and monchikites. Dark, glass-rich, with absent or almost absent plagioclase \pm nepheline, abound in clinopyroxene (zonal, diopside-augite in core to titanaugite in peripheries) and olivine. Sometimes contain microphenocrysts of biotite and barkevikite. All these components, with titaniferous iron ore minerals and clinopyroxene microlites including, are embedded in soda-rich glassy matrix. Calcite and analcite regularly occur in anhedral grains or infill voids (\pm chloropheite). This definition may be also attributed to the described West High Tatra limburgites and to some Silesian-Moravian teschenite formation rocks, appearing in Flysch (Outer) Zone of north-western Carpathians.

Formerly and lately mentioned, as other world occurrences of limburgites, seem to be geotectonically connected with circumcratonic rift and fracture zones, peculiar by reduced continental crust component. Such forms as domes testify to high viscosity of overcooled, slightly crystallized magmas, due to the deficiency of silica tetrahedrons. The viscosity rises abruptly with the loss of mineralizers, especially of CO_2 , main carrier of alkalis. These are in limburgites and augitites, basing on R.A. Daly's (1933) data, moderately represented judging from the ne norm values, ranging between 14 and 12 per cents, respectively. This constituted a.o. an argument for A. Streckeisen (1978) describing limburgite as a melahyal-

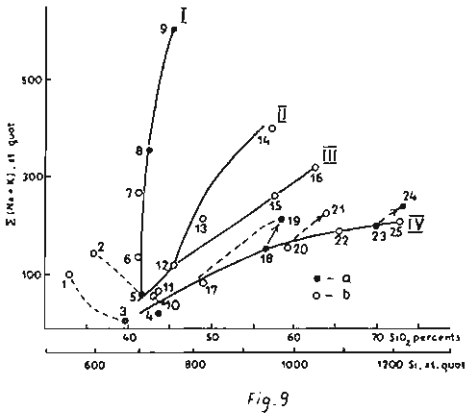


Fig. 9

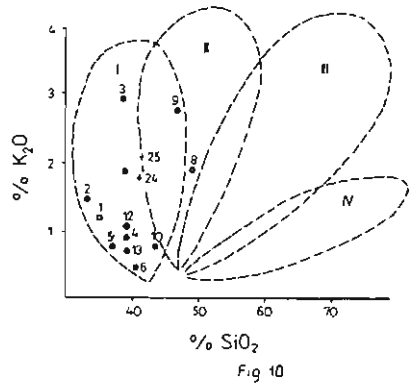


Fig. 10

Fig. 9. The main igneous rocks series, after L.S. Borodin et al. (1974); Na + K - Si diagram a little simplified

Główne serie skał magmowych według L.S. Borodina i. in. (1974); diagram Na + K - Si nieco uproszczony

I - alkaline ultrabasic, II - alkaline-gabbroidal (potassic and sodic-potassic), III - alkaline-gabbroidal (sodic), IV - granitoidal; numbers denote: 1 - alnoite, 2 - melilitite basaltoid, 3 - dunite, 4 - lherzolite, 5 - pyroxenite, 6 - limburgite, 7 - nephelinitic, 8 - ijolite, 9 - urtyt, 10 - porfiryrt pikrytowy, 11 - ankaramit, 12 - alkaline-olivine basalt, 13 - trachibasalt, 14 - fonolit, 15 - trachandezyt, 16 - alkaline trachyte, 17 - tholeiitic basalt, 18 - dioryt, 19 - syenit, 20 - andezyt, 21 - trachit, 22 - dacyt, 23 - granit, 24 - alkaline granite, 25 - rhyolit; a - plutonites, b - vulcanites

I - alkaliczno-ultrazasadowa, II - alkaliczno-gabbroidalna (potasowa i sodowo-potasowa), III - alkaliczno-gabbroidalna (sodowa), IV - granitoidowa; 1 - alnoit, 2 - bazaltoid melilitowy, 3 - dunit, 4 - lherzolit, 5 - proksenit, 6 - limburgit, 7 - nefelinit, 8 - ijolit, 9 - urtyt, 10 - porfiryrt pikrytowy, 11 - ankaramit, 12 - bazalt alkaliczno-oliwinowy, 13 - trachibasalt, 14 - fonolit, 15 - trachandezyt, 16 - trachit alkaliczny, 17 - bazalt toleitoowy, 18 - dioryt, 19 - syenit, 20 - andezyt, 21 - trachit, 22 - dacyt, 23 - granit, 24 - granit alkaliczny, 25 - ryolit; a - plutonity, b - wulkanity

Fig. 10. The K_2O versus SiO_2 diagram showing supposed relations of the differentiation trends of limburgite (I), shoshonitic (II), calc-alkaline (III) and tholeiitic (IV) magmas

Dyagram zależności K_2O od SiO_2 , ukazujący przypuszczalne zależności trendów dyferencjacji magm limburgitowych (I), shoshonitowych (II), wapienno-alkalicznych (III) i toleitoowych (IV)

24 i 25 - signify R.A. Daly's (1933) and Slovakian (D. Hovorka and J. Spišiak, 1981) limburgite averages, respectively; other explanations as given in Tables 1 and 2

24 i 25 - średnie limburgitów według R.A. Dally'ego (1933) i limburgitów słowackich (D. Hovorka, J. Spišiak, 1981); pozostałe objaśnienia jak w tab. 1 i 2

basanite. It is worth repeating J. Nicholl's et al. (1982) clause requiring over 5 per cent of ne norm as quantity needed for application of basanite term.

As far as present knowledge extends it is hard to deduce the provenance of limburgite magma. Yu.A. Kuznetsov (1964) reckons the limburgites among members of alkaline basaltoid magmatic formation. To the same formation includes L.S. Borodin et al. (1974) both, the limburgites and the augites, recording many old and new examples of their occurrences, bound to rifting phenomena. Likewise did also E.P. Saggerson (1970) studying East African Rift Valleys magmas (Fig. 8).

After Yu.A. Kuznetsov's opinion (*l. c.*) the limburgites could not only develop in the „shadow” of more spreaded alkaline-olivine basalt magmas but also as territorially independent. Among mineralogical features he emphasizes, a.o., titanogitic character of clinopyroxenes and lack of orthopyroxenes. Regarding geotectonic position he recognized as dominating factor of emplacement - large fractures, reaching great depths.

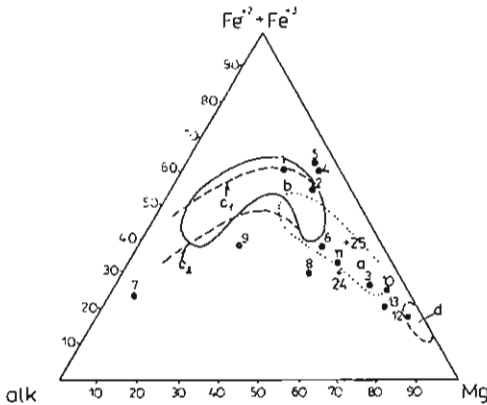


Fig. 11. Simplified R. Hekinian's and G. Thompson's (1976) triangular diagram demonstrating relations of examined rocks against Atlantic Rift Valley volcanics (a), aseismic ridges volcanics (b), tholeiitic basalts, e. g. Iceland (c_1) and alkaline basalts, e. g. Azores (c_2) differentiation courses, as well as Mid-Atlantic Range and fracture zones ultramafites (d)

Zmodyfikowany trójkątny diagram według R. Hekiniana i G. Thompsona (1976) ukazujący stosunki badanych skał do dróg dyferencjacji wulkanitów atlantyckiego ryftu (a), grzbietów asejsmicznych (b), bazaltów toleitytowych, np. Islandii (c_1) i bazaltów alkanicznych, np. Azorów (c_2) oraz do ultramafitów Grzbietu Śródatlantyckiego i stref przecławowych (d)

Explanations as given in Fig. 10

Objasnienia jak na fig. 10

Similar, deep in the mantle situated source regions are sometimes ascribed to komatiite magmas, which as limburgite magmas distinguish high values of CaO/Al_2O_3 proportion (≥ 1). It should not be inferred, however, that they have been originated in the same way. The komatiites are much more MgO -rich, SiO_2 -deficient and poor in incompatible (large-ion) elements pointing out high melting degree and/or degraded parental material. Extracted from mantle or even from lower (ultramafic) part of oceanic core they probably did not have any possibility to contamination with sialic material.

The limburgites, on the other hand, seem to be derivatives of local, small-scale melting in an environment rich still in fluid phase, particularly in carbon dioxide. This fluid component might be concentrated in limburgites and especially in kimberlites, playing an important role during their emplacement in higher, rigid regions of lithosphere. The carbon dioxide was also specially responsible for alkalis migration, as can be deduced from the co-occurrence of carbonatites with nephelinites, ijolites a.o. These products of fractional crystallization with or without metasomatism on the simplified L.S. Borodin's et al. (1974) alkalis - SiO_2 diagram (Fig. 9) are grouped within the limits of one, alkaline-ultrabasic (group 1) differentiation trend. The limburgites, characteristically, are one of the initial members of this trend. It should be also remarked that a similar, separate position this alkaline-ultrabasic trend with limburgites occupies in the $K_2O - SiO_2$ diagram (Fig. 10). Such distinctly incompatible element as potassium easily has been underwent, with or without fractionation, an influence of fluid transfer.

A well marked tendency of alkalis migration from recorded primary to differentiated magmas visualizes triangular diagram (Fig. 11), constructed by R. Hekinian and G. Thompson (1976) for oceanic crust volcanics. Beside the alkaline trend of differentiation an enrichment in iron, largely trivalent, in four examined samples (nos 1, 2, 4 and 5) should be noticed. This stays in connection with superficial, mostly hydrothermal, alterations, e.g. calcitization, which among other generated free-silica (compare Q norm in Fig. 2), and silica bound to smectites, chlorites and secondary albites. These hydrotogenic alteration processes might also be responsible for potassium decrease and titanium increase (Fig. 12). The latter, as chemically inert element, concentrates with iron in secondary products,

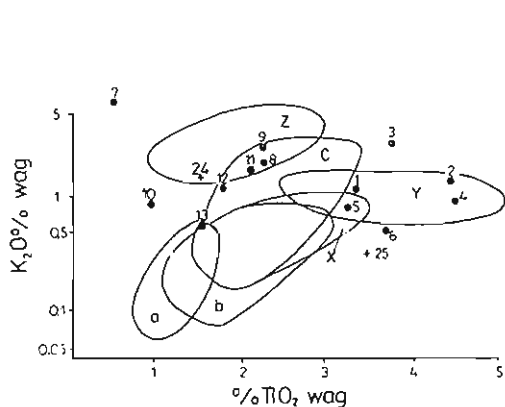


Fig 12

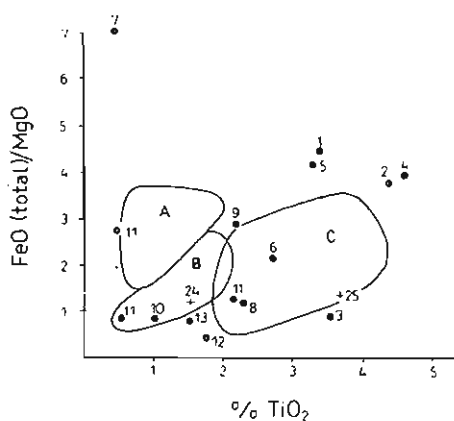


Fig 13

Fig. 12. The combined R. Hekinian's and G. Thompson's (1976) $K_2O - TiO_2$ diagram illustrating relations between examined rocks and M.A.R. Rift Valley rocks (a), fracture zone volcanics (b), aseismic ridge volcanics (c), tholeiites (X), alkali-basalts (Y) and differentiated rocks with SiO_2 over 51% (Z)

Diagram kombinowany, według R. Hekiniana i G. Thompsona (1976), $K_2O - TiO_2$ przedstawiający zależności między badanymi skałami i skałami środkowoatlantyckiego ryftu (a), wulkanitami stref przełamowych (b), wulkanitami grzbietów asejsmicznych (c), toleitami (X), bazaltami alkalicznymi (Y), skałami zróżnicowanymi z zawartością SiO_2 ponad 51% (Z)

Explanations as given in Fig. 10

Objaśnienia jak na fig. 10

Fig. 13. The W. Glassley's (1974) total $FeO/MgO - TiO_2$ diagram showing the position of examined rocks and variation fields of island-arch tholeiites (A), mid-oceanic range tholeiites (B) and ocean bottom basalts (C)

Diagram FeO całkowitego $/MgO - TiO_2$, według W. Glassleya (1974); pokazujący pozycję badanych skał i pola zmienności toleitów luków wyspowych (A), toleitów grzbietów śródoceanicznych (B) i bazaltów dna oceanicznego (C).

Explanations as given in Fig. 10

Objaśnienia jak na fig. 10

creating badly defined mineral, called leucoxene. Noteworthy, is also the accumulation of plotted projection points in or in vicinity of fields belonging to the alkaline basalts (Y) and differentiated rocks (Z).

Some further indications regarding consanguinity of reported rocks and secondary iron increase (samples nos 1, 2, 4 and 5) presents another diagram demonstrating total $FeO/MgO - TiO_2$ relations (Fig. 13).

For the provenance speculations such microelements as nickel and chromium are undoubtedly more convenient than major elements. Both are considered as good indicators of the mantle parental material content in undifferentiated magmas. Comparison of Niggli's mg parameter with Ni and Cr contents (Fig. 6, see also Figs 5 and 7) reveals relatively high concentrations, especially if one takes into account some impoverishment caused by calcitization (compare position of 2-2a, 1-1a, 4, 5 plots with 3) and other formerly mentioned redistribution phenomena. Limburgite porphyries (samples 10 and 13) of teschenite formation differ conspicuously due to fractional crystallization in the picrite direction (mafitic cumulates).

Postulated by D. Hovorka, J. Spišiak (1981) genetical liason of limburgites with ocean island volcanism is much problematic. Small content of magnesium and high Ca/Al values together with abundance of incompatible elements as K and Ti prove the appurtenance of limburgites to the volcanics bound to circumcratonic rifting phenomena. Analogical geotectonic conditions as those accompanying the formation of Late Jurassic-Cretaceous Carpathian embryonal geosyncline (Kay's tectogene) and similar magmatic rock formations can be found in many examples of rifting, originated in the past and now forming. Some approach to the scale of Neocimmerian tectonic movements which took place during emplacement of discussed Carpathian initialites gives their repartition. They are reported as far as Silesian nappe of External (Flysch) Carpathians in the north and as the Gerečse Mountains in the south.

Acknowledgment: The authors are indebted to prof. W. Ryka for making available the samples of High Tatra limburgites used in this study.

Translated by T. Wieser

Oddział Karpacki
Instytutu Geologicznego
Kraków, Skrzatów 1
Received: 18 IX 1984

REFERENCES

- ALEXANDROWICZ S.W., HEFLIK W. (1974) – Żyła cieszynitowa w molasowych osadach miocenu w Bacharowicach. *Kwart. Geol.*, **18**, p. 925–926, nr 4.
- ALEXANDROWICZ S.W., HEFLIK W., WIESER T. (1978) – Bloki law i hyaloklastytów w górnym miocenie (baden dolny) Bacharowic. *Symposium naukowe nt.: „Pozycja stratygraficzna cieszynitów i warunki ich występowania”*. Materiały pod red. W. Nowaka i T. Wiesera, Kraków.
- BARTH T. (1948) – Oxygen in rocks: a basis for petrographic calculation. *Jour. Geol.*, **56**, p. 50–60, nr 1.
- DALY R.A. (1933) – *Igneous rocks and the depths of the Earth*. Mc Graw-Hill, New York.
- GLASSLEY W. (1974) – Geochemistry and tectonics of the crescent volcanic rocks, Olympic Peninsula, Washington. *Bull. Geol. Soc. Amer.*, **85**, p. 785–794, nr 5.
- HEKINIAN R., THOMPSON G. (1976) – Comparative geochemistry of volcanics from Rift Valleys, Transform Faults and Aseismic Ridges. *Contr. Miner. Petrol.*, **57**, p. 145–162.
- HOVORKA D. (1976) – Predtercierne formacie bazitov Zapadnych Karpat. *Miner. Slov.*, **8**, p. 113–133, nr 2.
- HOVORKA D., SPIŠIAK J. (1981) – Hyalobazanity (limburgity) Osobitej v Tatrach. W: *Paleovulkanizmus Zapadnych Karpat*. Pr. zbiorowa pod red. S. Bajonika i D. Hovorki, p. 145–155. Bratislava.
- KOTAŃSKI Z., RADWAŃSKI A. (1959) – Fauna z *Pygope dipha* i limburgity w tytonie wierchowym Osobitej. *Acta Geol. Pol.*, **9**, p. 519–534, nr 4.
- KREUTZ S. (1913) – O limburgicie w Tatrach. *Rozpr. PAU A53* (ser. III, 13), p. 57–79.
- KUNO H., YAMASAKI K., JIDA C., NAHASHIMA K. (1957) – Differentiation of Hawaiian magmas. *Jap. Jour. Geol. Geogr.*, **28**, nr 4.
- LEFELD J. (1968) – Stratygrafia i paleogeografia dolnej kredy wierchowej Tatr. *Studia Geol. Pol.*, **24**.

- MAHMOOD A. (1973) – Petrology of the teschenitic rocks series from the type area of Cieszyn (Teschen) in the Polish Carpathians. *Rocz. Pol. Tow. Geol.*, **43**, p. 153–226, z. 2.
- MOROZEWICZ J. (1912) – Księga Pam. XI Zjazdu Lek. i Przyr. w Krakowie, p. 221.
- NICHOLLS J., STAUT M.Z., FIESINGER D.W. (1982) – Petrologic variations in Quaternary volcanic rocks, British Columbia and the nature of the underlying Upper Mantle. *Contr. Miner. Petrol.*, **79**, p. 201–218.
- NIGGLI P. (1936) – Über Molekularnormen zur Gesteinsberechnung. *Schw. Miner. Petrogr. Mitt.*, **16**.
- PACAK O. (1926) – Sopečné horniny na severním upati Bezkyd Moravských. *Česka Akad. Ved. a Umeni. Praha-*
- POLAŃSKI A., SMULIKOWSKI K. (1969) – *Geochemia*. Wyd. Geol. Warszawa.
- POLDERVAART A., HESS H. (1951) – Pyroxenes in the crystallization of basaltic magma. *Jour. Geol.*, **59**, p. 172–178.
- RABOWSKI F. (1930) – O pochodzeniu limburgitów tatrzańskich i stosunku wzajemnym płaszczowin wyodrębnionych między pasmem Skałek a górami Veporu. *Spraw. PIG*, **6**, p. 212–222, z. 1.
- SAGGERSON E.P. (1970) – The structural control and genesis of alkaline rocks in Central Kenya. *Bull. Volcan.*, **34**, p. 38–76, nr 1.
- SMULIKOWSKI K. (1929) – Materiały do znajomości skał magmowych Śląska Cieszyńskiego. *Arch. Nauk. Lwów*, **5**, p. 1–124.
- STRECKEISEN A. (1978) – Classification and nomenclature of volcanic rocks, lamprophyres, carbonates and melilitic rocks. *Neues Jahr. Miner. Abh.*, **134**, p. 1–14, nr 1.
- STRZĘPKA J., ŚLĄCZKA A., WIESER T. (1978) – Otoczaki cieszynitów w dolnym miocenie w otworze Sucha I. *Sympozjum naukowe nt.: „Pozycja stratygraficzna cieszynitów i warunki ich występowania”*. Materiały pod red. W. Nowaka i T. Wiesera. Kraków.
- UHLIG V. (1897) – Geologische Karte des Tatragebirges I–IV. *Denkschr. d. Math.-Mat. Kl. d. Kais. Ak. Wiss.*, p. 64–68.
- ZORKOVSKY V. (1949) – Bazické efuziva v mezozoiku zapadneho a stredneho Slovenska. *Pr. Stat. Geol. Ust.*, **26**, p. 1–40.
- БОРОДИН Л.С. и др. (1974) – Главнейшие провинции и формации щелочных пород. АН СССР. Инст. Мин. Геох. и Кристаллохимии Редких Элементов. Изд. Недрa Москва.
- КУЗНЕЦОВ Ю.А. (1964) – Главные типы магматических формаций. Москва.

Ирена ГУЦВА, Тадеуш ВЕСЕР

ЛИМБУРГИТЫ В ПОЛЬСКИХ КАРПАТАХ

Резюме

Геохимическая и петрографическая корреляция лимбургитоподобных пород Силезско-Моравской цешинитовой свиты с лимбургитами Западных Высоких Татр выявила их сходство. Эти зачатки являются продуктом начальной стадии образования рифта во время неокиммерийских движений, сыгравших решающую роль в образовании тектогена флишевых Карпат.

Химизм и геотектоническое положение аналогичны другим известным лимбургитовым магмам, изливающимся в пределах новых рифтовых долин и больших околократонных разломов при уменьшенной мощности континентального покрова.

Остальные породы цешинитовой свиты: это частичные магмы, продукты дифференциации первичной магмы покровного происхождения, химически сходной с пимбургитовой магмой.

Несмотря на высокую вязкость ультрамафитовых пимбургитовых магм, часть их благодаря высокому давлению флюидов и газов (особенно CO_2) смогла вырваться на земную поверхность на дне морей. Таким путем образовались в разной степени вторично преобразованные лавы и чаще встречающиеся гиалокластиты.

Irena GUCWA, Tadeusz WIESER

LIMBURGITY W POLSKICH KARPATACH

Streszczenie

Geochemiczna i petrograficzna korelacja skał limburgitopodobnych śląsko-morawskiej formacji cieszyńskiej z limburgitami zachodnich Tatr Wysokich wykazała ich ściśle pokrewieństwo. Te inicjalne są wynikiem początkowego riflingu związanego z ruchami neokimeryjskimi, decydującymi o powstaniu tektonogenu Karpat fliszowych.

Zarówno chemizm, jak i sytuacja geotektoniczna są analogiczne do innych, znanych wystąpień magm limburgitowych, wydobywających się w obrębie nowopowstałych dolin ryflowych i dużych rozłamów wokółkratonicznych, przy zredukowanej miąższości skorupy kontynentalnej.

Pozostałe skały formacji cieszyńskiej są magmami cząstkowymi, produktami dyferencjacji pierwotnej magmy pochodzącej z płaszcza, chemicznie zbliżonej do magmy limburgitowej.

Mimo wysokiej lepkości ultramaficznych magm limburgitowych, część z nich wskutek wysokiej prężności fluidów i gazów (zwłaszcza CO_2) zdołała wydobyć się na powierzchnię Ziemi w warunkach podmorskich. Tą drogą powstawały zarówno lawy, jak i częstsze od nich hyaloklaasty, różnie wtórnie przeobrażone.

TABLE I

Fig. 14. Glomerophytic aggregations of augite (upper part) and discoidal amygdale consisting of albite in amygdaloidal limburgite from Bobrowiecka Pass. Sample no. 1, $\times 70$, crossed nicols

Wydzielenia glomerofityczne augitu (górną część) i dyskooidalny „migdał”, złożony z albitu w migdałowcym limburgicie z Przełęczą Bobrowieckiej. Próbkę nr 1, pow. $70 \times$, nikole skrzyżowane

Fig. 15. Vesicles filled with albite (largest one with chlorophite rim) chlorophite and septechlorite (small one with albite crystals growing inwards), as well as with calcite (upper left corner) in amygdaloidal limburgite from Osobita. Sample no. 2, $\times 70$, crossed nicols

Wakuole wypełnione albitem (największe, z chlorofeitymowym rąbkim), chlorofeitem i septechlorytem (drobne z kryształami albitu rosnącymi do wewnątrz) oraz z kalcytem (górną lewą część) w migdałowcym limburgicie z Osobitej. Próbkę nr 2, pow. $70 \times$, nikole skrzyżowane



Fig. 14

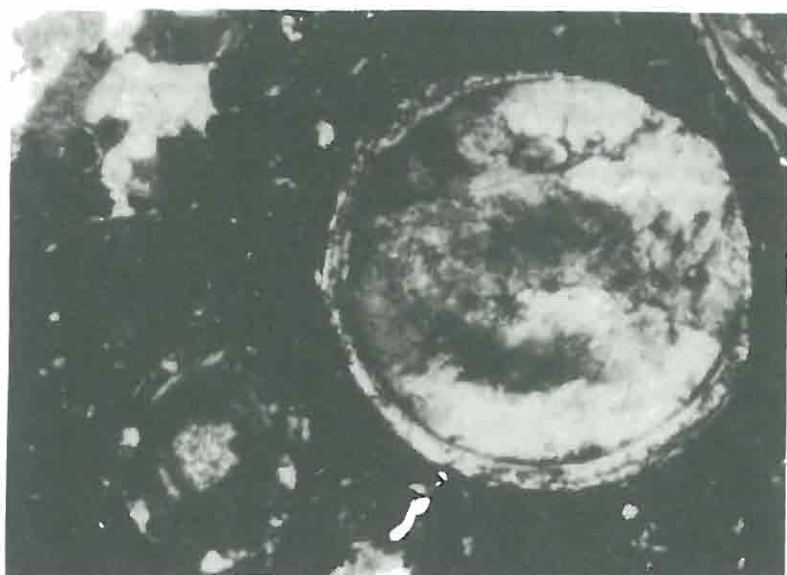


Fig. 15

TABLE II

Fig. 16. Limburgite from Bacharowice with mineral composition and structural-textural features transitional to monchikite. Visible saponitized olivine phenocryst (upper right), small pheno- and microphenocrysts of augite (clear areas) and elongated microlites of biotite and apatite. Sample no. 3, $\times 24$, without nicols

Limburgit z Bacharowic o składzie mineralnym i cechach strukturalno-teksturalnych przejściowych do monchikitu. Widoczne saponityzowane fenokryształy oliwinu (prawa góra), drobne feno- i mikrofenokryształy augitu (jasne obszary) oraz wydłużone mikrolity biotytu i apatytu. Próbką nr 3, pow. 24 \times , bez nikoli

Fig. 17. Amygdaloidal limburgite- or better augitite-like rock from Bacharowice exhibiting large vesicles filled with calcite and smaller ones — with zonary smectite (nontronite in darker zones and montmorillonite in clearer zones). Sample no. 5, $\times 16$, without nicols

Skala migdałowcowa limburgito- lub augitytopodobna z Bacharowic, z dużymi pęcherzami wypełnionymi kalcjtem lub drobniejszymi — pasowym smektytem (nontronit w ciemnych pasach i montmorillonit w jasnych). Próbką nr 5, pow. 16 \times , bez nikoli

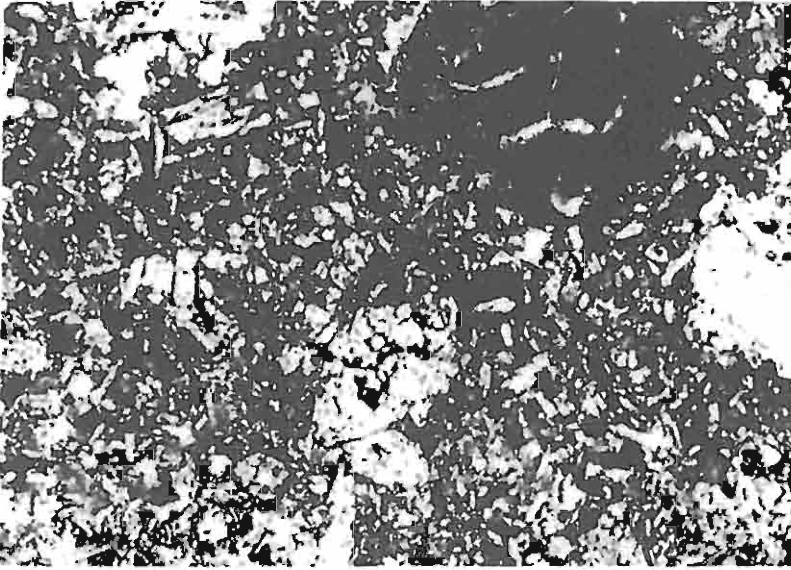


Fig. 16

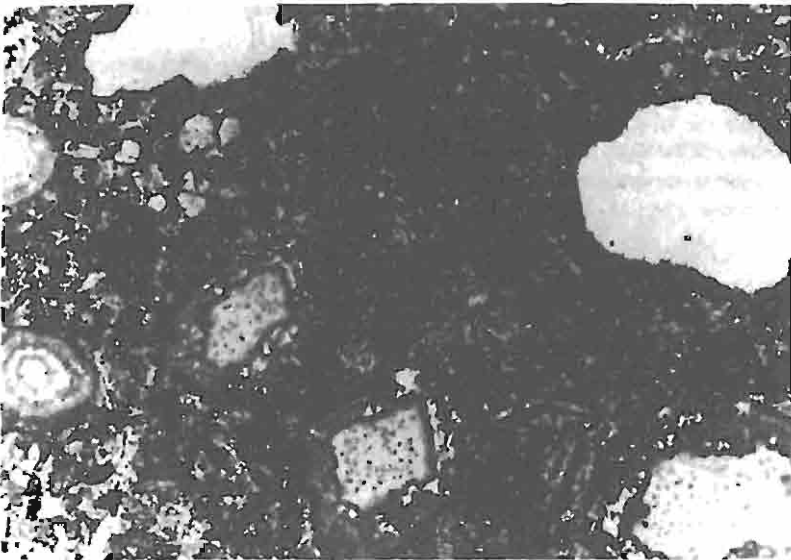


Fig. 17

TABLE III

Fig. 18. Fine-grained limburgite hyaloclastite, composed of chloritized as well as smectitized glass particles and rarer rhombohedral crystals of authigenic calcite in marly matrix. Found in Bacharowice with formerly mentioned augite-like amygdaloid. $\times 28$, without nicols

Drobnoziarnisty białoklastyt limburgitowy, złożony z chlorytyzowanych i smektyzowanych cząstek szkliska i rzadszych kryształów romboedrycznych kalcytu autigenicznego w marglistej matrix. Okaz znaleziony w Bacharowicach z poprzednio wspomnianym migdałowcem augitopodobnym. Pow. $28 \times$, bez nikoli

Fig. 19. Vesicles filled with calcite in lava breccia having composition and structural-textural features own to limburgite- or augite-like rocks. Found in borehole core Sucha IG 1 at 2818.35 m depth in Miocene deposits. Sample no. 4, $\times 11$, without nicols

Pęcherze wypełnione kalcytem w brekcji lawowej, mającej skład i cechy strukturalno-teksturalne właściwe skałom limburgito- i augitytopodobnym. Próbką nr 4 z głęb. 2818,35 m z otworu wiertniczego Sucha IG 1 z osadów miocenu. Pow. $11 \times$, bez nikoli

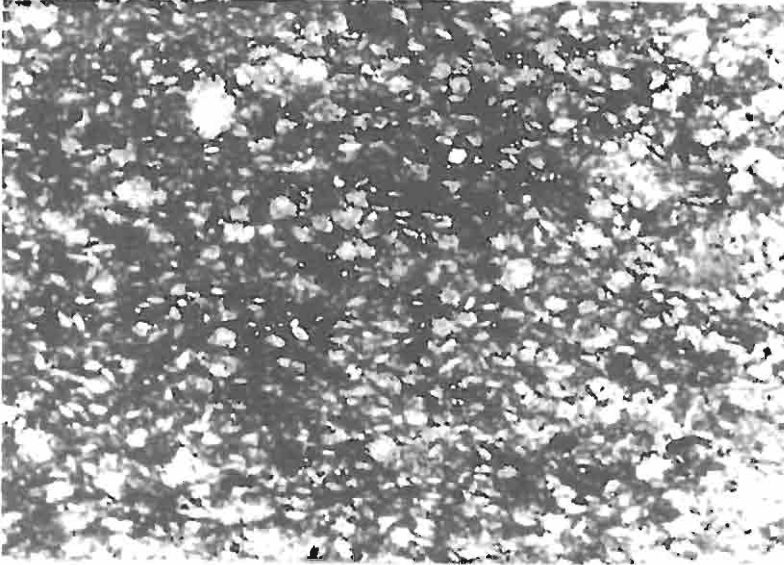


Fig. 18

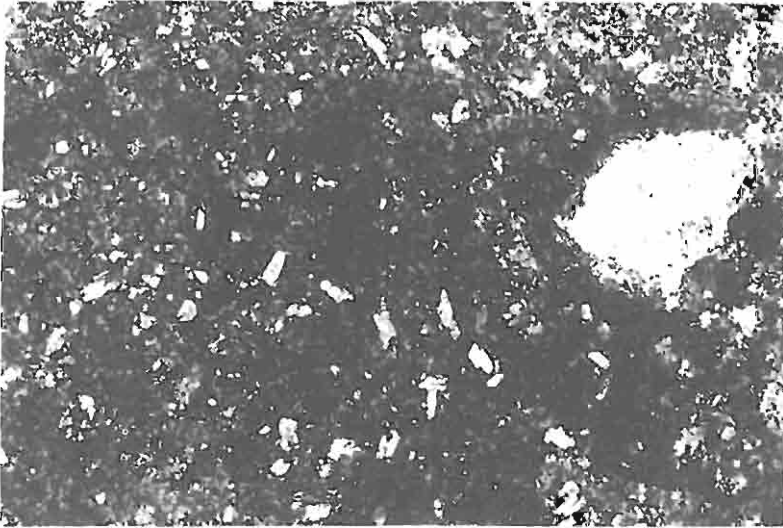


Fig. 19